AIAA JOURNAL
Vol. 35, No. 9, September 1997

Composite Patch Repairs of Metal Structures: Adhesive Nonlinearity, Thermal Cycling, and Debonding

Wai Tuck Chow* and Satya N. Atluri†
Georgia Institute of Technology, Atlanta, Georgia 30332-0356

Comparison with the experimental data has been carried out to determine the ability of the finite element alternating method in predicting the fatigue response of a cracked metallic panel with a partially debonded composite patch. A total of 15 different specimens are considered in this comparison. Some of the parameters that are varied in these specimens include the disbond location, the disbond area, the initial crack length, the maximum stress loading, and the stress ratio. For all of these specimens, it has been found that the numerical results correlate very well with the experimental data when the adhesive nonlinearity is properly accounted for in the analysis. In addition to this comparison with the experimental data, numerical studies have been carried out to examine the effect of the thermal cycling on the fatigue response of a bonded repair. It was found that, due to the strong difference in the thermal expansion coefficient of the boron/epoxy patch and the aluminum panel, the fatigue life of a specimen, which undergoes cycles of high stress at low-temperature and low stress at high-temperature loading, is dramatically reduced. It was also found that the fatigue life of a specimen that undergoes a thermal-mechanical-fatigue cycle is more sensitive to disbonds in the adhesive layer than a similar specimen that undergoes mechanical fatigue loading at a constant temperature. In addition to this study, numerical analysis has been carried out to study the interaction between two nearby composite patches. The study found very little interaction between the two patches when these two patches lie next to each other, with both the cracks under the patches being collinear and both being normal to the direction of the load. On the other hand, when the two patches lie vertical to each other, i.e., when the two cracks under the patches are parallel and one being on the top of the other, both the cracks being normal to the direction of the load, the fatigue life of this specimen can increase substantially when these two patches are very close to each other; however, this may lead to failure of the metal in between the patches, but this is not considered in the present study.

Introduction

A STUDY in predicting fatigue response of a cracked metallic panel has been conducted comparing experimental data obtained by Denney[1] to the finite element alternating method. As a result of the high replacement costs and shrinking budgets for aircraft acquisitions, many of the airplanes in the commercial as well as the military fleet are used beyond their original design lives. Consequently, these aircraft undergo high cycles of repeated pressurization and loading, which cause fatigue cracks to develop at regions of stress concentration in the structure. To enhance the life of an aging aircraft structure, the application of minor repairs using mechanically fastened metallic doublers, or adhesively bonded composite patches, becomes an increasingly important option in the aerospace industry. Although many of the repairs on an aircraft structure are still performed using mechanically fastened metallic doublers, various commercial airlines as well as military facilities have begun experimenting with repairs using adhesively bonded composite patches.[2] Repair using the metallic doubler requires the cracked portion to be cutout and replaced with an undamaged sheet. In contrast, bonded repairs offer a wide range of advantages such as ease of application, with no damage to the underlying structure. In addition, bonded repairs using laminated composites offer high stiffness to weight ratio, and such repairs can be readily formed into various complex shapes of different aircraft components. Nonetheless, some of the critical issues associated with the use of adhesively bonded composite patch repairs are still not fully resolved. These issues include the ability to predict the fatigue growth of cracks under the bonded composite patch as well as the effect of disbond of the patch on the effectiveness of the repairs.

Received Jan. 15, 1997; revision received June 4, 1997; accepted for publication June 4, 1997.

*Postdoctoral Fellow, Computational Modeling Center.
†Institute Professor, Regents' Professor of Engineering, Hightower Chair in Engineering, and Director, Computational Modeling Center. Fellow AIAA.

In general, the analysis of fatigue crack growth in the presence of composite patch repairs can be broadly categorized as either analytical or numerical. Based on the elastic inclusion analogy, Rose[3] has obtained the solution for long strip type patches by using a successive approximation method to deduce the asymptotic behavior of the modeled Fredholm integral equation. Rose[4] further extended this method to obtain an approximate solution for a crack inside an elliptical patch. The solution for the elliptical patch is further extended by Fredell[5] to include the effect of temperature. Although the solution for Rose's model[4,5] is simple and easy to implement, these solutions have strong limitations. Some of the limitations of Rose's model arise from the following assumptions. 1) The patch has to be either an infinite strip type or an elliptical shape type. 2) The material behavior for the adhesive layer is linear elastic. 3) The load transfer length must be significantly smaller than the patch size, i.e., the adhesive must be relatively stiff, or the size of the patch must be significantly large. 4) The bonding of the patch is perfect without disbonds. 5) The size of crack is small compared to the size of the patch. All of these assumptions limit the ability of Rose's model[4,5] to adequately analyze the effectiveness of most practical composite patches in reducing the fatigue crack growth. Therefore, to overcome these limitations, numerical methods have been employed in analyzing the effectiveness of repairs using composite patches. Jones and Callinan,[2] Mitchell et al.,[6] and Chu and Ko[7] have used the finite element method to study bonded patch repairs. Tarn and Shek[8] have combined the boundary element method (for the base metallic plate) and finite element method (for the patch) to estimate the stress intensity factors. Park et al.[9] have applied the integral equation approach in conjunction with the Schwartz–Neumann alternating method to calculate the stress intensity factors for cracks repaired with composite patches. In extending this work, the approach of the finite element alternating method was applied by Nagaswamy et al.[10] to model composite patches on a curved fuselage panel where the stress distributions due to curvature as well as the presence of stiffeners are accounted for. A comprehensive account of the analysis of adhesively bonded composite patch repairs, and the effects of various parameters in

the design of such patches, is given in the monograph by Atluri.[21] Although these studies provide the methods to analyze a composite patch with perfect adhesive bonding, there have been few studies that concentrate on the verification of numerical analysis against experimental results especially when disbonds between the metallic sheet and the composite patch exist.

Roderick[11] has examined the cyclic growth of a crack inside an elliptical disbond of a composite patch. Baker[12] has studied experimentally the effectiveness of composite repairs with disbond that occur during manufacturing. Denney[1] has experimentally investigated the fatigue life of a cracked metallic specimen with a composite patch and with intentional disbonds of various locations and sizes. This experiment also studies the effect of initial crack length, maximum applied fatigue stress, and stress ratio. In this paper, analyses are performed using the finite element alternating method (FEAM) to study the fatigue life of a crack in a metallic specimen with partially disbonded composite patches, under different loading conditions. These numerical results are compared with the experimental data obtained by Denney[1] to determine the ability of FEAM in predicting the fatigue life of cracked metallic specimens with partially disbonded composite patches. Because debonds in bonded repairs are found frequently and the replacement of defective patches remains very difficult, the ability to predict the fatigue characteristics of partially debonded patches would be an extremely important issue to be resolved before bonded repairs can be used widely in the aerospace industry. In addition to the comparison with the experimental results, this paper also evaluates the effects of 1) temperature cycles, 2) initial stresses due to the curing of the patch, and 3) adhesive nonlinearity, on the fatigue characteristics of partially bonded patches. Furthermore, the interaction of two neighboring composite patches is also studied.

FEAM

Through a series of papers by Nishioka and Atluri,[13] Atluri and Nishioka,[14] Rajiyah and Atluri,[15] Park and Atluri,[16] and Wang and Atluri,[17] the alternating method has been established as an effective method in calculating the stress intensity factors for two- and three-dimensional linear elastic fracture mechanics. The cost effectiveness of this method is achieved by combining the numerical methods such as the boundary element method or the finite element method for analyzing only an uncracked structure, with the analytical solutions of multiple collinear cracks. Because the analytical solutions for the cracks are incorporated directly into the alternating method, the cracks do not need to be meshed in the finite element model. Hence, a very fine mesh, which is typically required for a direct numerical analysis of a linear elastic fracture mechanics problem, would not be required in the present finite element alternating method. For this reason, the computational time as well as the time needed to prepare the finite element mesh are substantially reduced.

In the Schwartz–Neumann alternating method, two solutions are required. Solution 1 is a general analytical solution for an embedded crack in an infinite domain subjected to arbitrary crack surface traction. Solution 2 is a numerical scheme (the finite element method in this paper) to solve for the stresses in an uncracked finite body.

The general solution for an embedded line crack in a two-dimensional infinite body is given by Muskhelishvili[18] in terms of complex potential functions. To apply this solution in the alternating method, Park and Atluri[16] used a set of delta functions to represent the crack surface traction to analytically solve for the Cauchy integral required for the complex potential functions. To improve the accuracy, Park[19] used a set of approximate piecewise constant functions. In this paper, the crack surface traction is represented by a set of approximate linear basis functions, the corresponding analytical solution for which was developed by Wang and Atluri.[17] The stress intensity factors at the crack tips can then be directly calculated from the coefficients of the linear basis functions.

The finite element solution involves the analysis of the uncracked finite domain to calculate the stresses at the location of the actual cracks. Because the surface of each crack is traction free in the actual problem, these stresses are removed by applying the reverse tractions on the crack face, and the analytical solution is then used to compute the K-factors corresponding to these reversed tractions. As explained subsequently, this procedure will have to be repeated several times until convergence of the solution is achieved. The detailed steps involved in the FEAM for an embedded crack in a finite body now follow, with steps 2–6 representing the iterative loop.

1) Solve the uncracked finite body under the prescribed tractions and displacements using the finite element method. This finite body has the same geometry as the original problem, except that the crack is ignored.

2) Using the finite element solution, a fit based on piecewise linear functions is made for the residual tractions at the crack surface location.

3) The residual tractions obtained in the preceding step are reversed to create a traction free crack face as in the given problem.

4) Using the reversed piecewise linear tractions, the analytical solution to the infinite body problem is solved.

5) The stress intensity factors for the current iteration are calculated using the piecewise linear solution. If the magnitude of the stress intensity factors is less than a prescribed tolerance, then it is assumed that convergence has been achieved and the analysis is completed.

6) The tractions and displacements at the boundaries of the finite body are calculated. To satisfy the prescribed traction and displacement boundary conditions, the residual tractions and displacements on the external boundary are reversed. Using the reversed loading, the procedure would return to step 2.

In practice, it has been found that this iterative procedure converges in less than five iterations in most cases. The overall stress intensity factors of the original problem are obtained by summing the stress intensity factors for all iterations. Note that the finite element method is used only to obtain a solution for the uncracked problem; hence, the FEAM is very effective from the computational point of view, particularly for fatigue growth analysis. This is because the finite element stiffness matrix is decomposed only once and the decomposed matrix can be used repeatedly for all iterations as well as different crack lengths.

Implementation of Composite Patch Analysis

The aim is to demonstrate the ability of the FEAM in predicting the fatigue response of a cracked panel with a partially disbonded composite patch. For the present study, numerical analysis has been carried out to model the experiment performed by Denney[1] on partially disbonded composite repairs. In the experiment,[1] the patch (made of three plies of unidirectional boron/epoxy laminate) is bonded to a 2024-T3 aluminum panel with AF-163-2 film adhesive. The geometries of the composite patch and the aluminum panel are given in Fig. 1. The material properties of the boron/epoxy laminate, the aluminum panel and the adhesive layer are given in Table 1. In the current analysis, the patch and the panel are modeled with eight-noded isoparametric plane stress elements. The adhesive film is modeled with isoparametric 16-noded adhesive elements developed by Chu and Ko.[7] The adhesive element is based on a linear elastic relationship between the shear stress and the difference of displacements between the patch and the panel:

$$\tau = K_{\mathrm{ADHE}}(u_{\mathrm{patch}} - u_{\mathrm{panel}}) \tag{1}$$

where

$$K_{\mathrm{ADHE}} = \left[\frac{t_{\mathrm{adhe}}}{G_{\mathrm{adhe}}} + \frac{3}{8}\left(\frac{t_{\mathrm{patch}}}{G_{\mathrm{patch}}} + \frac{t_{\mathrm{panel}}}{G_{\mathrm{panel}}}\right)\right]^{-1} \tag{2}$$

Here u is the displacement, t is the thickness, and G is the shear modulus. In general, the adhesive material can behave in a very nonlinear fashion. This nonlinear behavior can be modeled by

Table 1 Material properties for the aluminum panel, the boron/epoxy patch, and the adhesive layer

Material	$E_L/E_T/G$, GPa	Poisson ratio	CTE α_L, 10^{-6}/°C	Thickness, mm
2024-T3	72.4/72.4/27.2	0.33	22.7	1
Boron/epoxy	210/25/72.4	0.168	4.5	0.127
AF-163-2	NA/NA/0.405	——	——	0.127

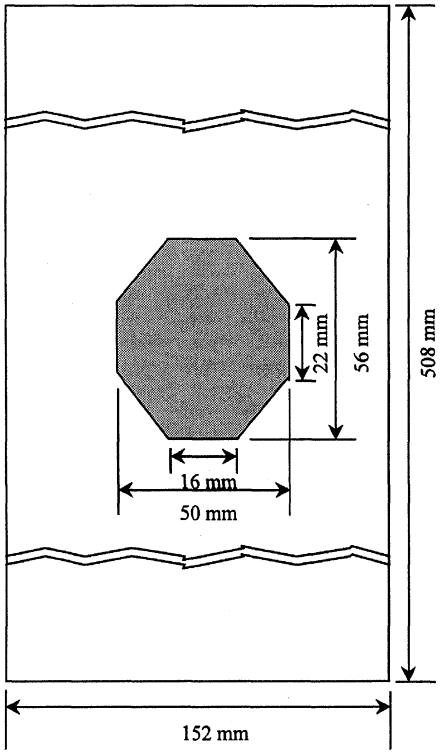

Fig. 1 Geometry of the aluminum patch with the boron/epoxy patch.

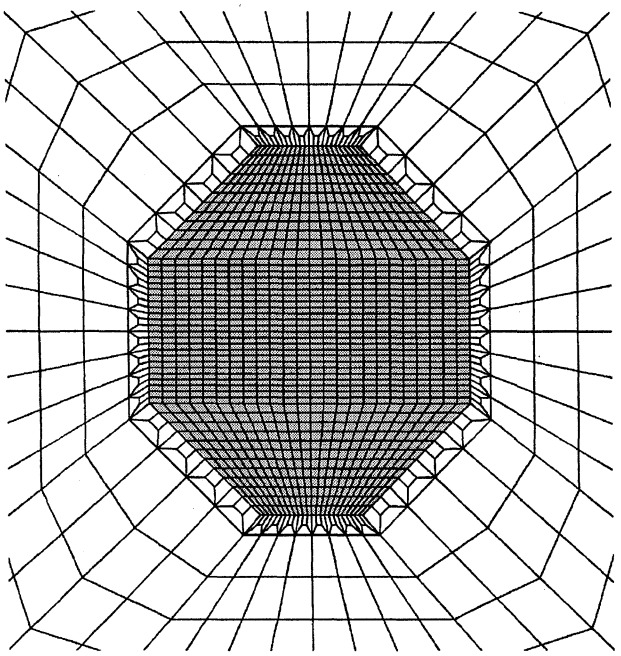

Fig. 2 Finite element mesh of the composite patch on the aluminum panel.

an elastic–plastic constitutive law, with a possible rate dependence. Thus, a fully nonlinear analysis of the metallic-plate/adhesive layer/composite patch system with 1) linear elastic modeling of the metallic plate and the patch and 2) elastic–plastic modeling of the adhesive layer may, in general, be necessary. However, for ease of use of the analytical methodology in practical situations, only a fully linear analysis of the metallic plate/adhesive layer/patch system is preferable. To account for the adhesive nonlinearity in the context of this fully linear analysis, however, the tangent modulus G_{adhe} is chosen as the slope of the nonlinear shear stress–shear strain relation of the adhesive material at the current level of shear stress in the adhesive layer.

The finite element mesh for the composite patch on the aluminum panel is shown in Fig. 2. The mesh contains 4176 elements and 9337 nodes. To calculate the stress intensity factors of a cracked panel under the composite patch, two steps are involved. In the first step, the crack in the panel along with the composite patch and the adhesive layer are explicitly modeled in the finite element mesh. From the finite element solution, the shear stress in the adhesive layer is calculated using Eq. (1). In the second step, the stress intensity factors of the cracked panel are solved using the FEAM, which uses the same finite element mesh except that the crack is not modeled explicitly. The shear traction on the cracked panel (transferred through the adhesive layer) calculated in step 1 is converted to nodal force to be applied in step 2. Because this shear traction accounts for the closing force of the composite patch, only the cracked panel is required to be modeled in step 2. Note that, because the FEAM is used in step 2, a very fine mesh near the crack tip is not required.

The fatigue growth of a crack in general can be calculated as a function of loading cycles. To take into account the effect of stress ratio, the Forman's crack growth equation[20] is used. This equation is given as

$$\frac{da}{dN} = \frac{C(\Delta K)^n}{(1-R)K_C - \Delta K} \tag{3}$$

Here a is the crack length, N is the number loading cycles, ΔK is the range of the equivalent stress intensity factor, and R is the stress ratio in the cyclic loading. For 2024-T3 aluminum alloy, the values of $K_C = 91\ \text{MNm}^{-3/2}(83{,}000\ \text{psi}\sqrt{\text{in.}})$, $C = 6.3 \times 10^{-21}\ \text{Pa}^{-2}(3 \times 10^{-13}\ \text{psi}^{-2})$, and $n = 3$ are used as suggested in Ref. 20. In general, a fatigue calculation involves the calculation of the number of cycles for a crack to grow to a specified length. Using a simple linear integration scheme to solve for Eq. (3), the fatigue life cycle of the crack is subdivided into a number of interval steps based on the finite element mesh. The total number of cycles is obtained by summing the values from each step.

To account for the temperature effect during the curing process, two analyses are required for each interval step of the fatigue crack growth analysis: one for the load applied at $\sigma_{\min}$ and the other is for the load applied at $\sigma_{\max}$. In the numerical model, it is assumed that the cure would fully solidify at 121°C and that the specimen would undergo fatigue cycling between $\sigma_{\min}$ (at temperature T_1) and $\sigma_{\max}$ (at temperature T_2). Because of the difference in the coefficients of thermal expansion α_L between the boron/epoxy patch and the aluminum panel, residual stresses would be induced in the repaired area when the temperature of the specimen differs from the cure temperature. And these residual stresses, which are dependent on the temperature of the specimen, would be superimposed on the mechanical loading applied on the specimen. Hence, in this numerical model, both the mechanical loading and the loading induced by thermal cycling are accounted for in the fatigue crack growth analysis. Note here that, even if the specimen were to undergo fatigue cycling at a constant temperature where $T_1 = T_2$ (which is the case in the comparison analysis with the experiment performed by Denney[1]), the drop in temperature after the curing process must be accounted for to properly model the fatigue crack growth of the specimens. Even though ΔK is not effected by the temperature drop after the curing process (because the fatigue cycle is at a constant temperature), the ratio of stress intensity factor, $R = K_{\min}/K_{\max}$, would be affected by this temperature drop. Because the boron/epoxy patch has a much smaller α_L than the aluminum panel, the patch contracts much less than the panel when the temperature drops. The residual stresses thus generated would cause the crack surface to open, resulting in a higher stress intensity factor and, hence, a higher stress ratio R. This higher stress ratio R would cause a faster crack growth as seen from Forman's crack growth equation[20] [Eq. (3)].

Results

Comparison of Numerical Result with Experimental Data

This study involves the analyses of four different intentional disbond configurations: a completely bonded patch (CBP) (Fig. 3a), crack tip disbonds (CTD) at both ends of the crack (Fig. 3b), a center disbond (CD) over the crack length (Fig. 3c), and a full width disbond (FWD) extending the full width of the patch and covering the crack (Fig. 3d). In some of these configurations, disbond areas of 20, 10, and 5% of the total bond area of the patch were investigated. These specimens would undergo fatigue cycling at room temperature, 20°C.

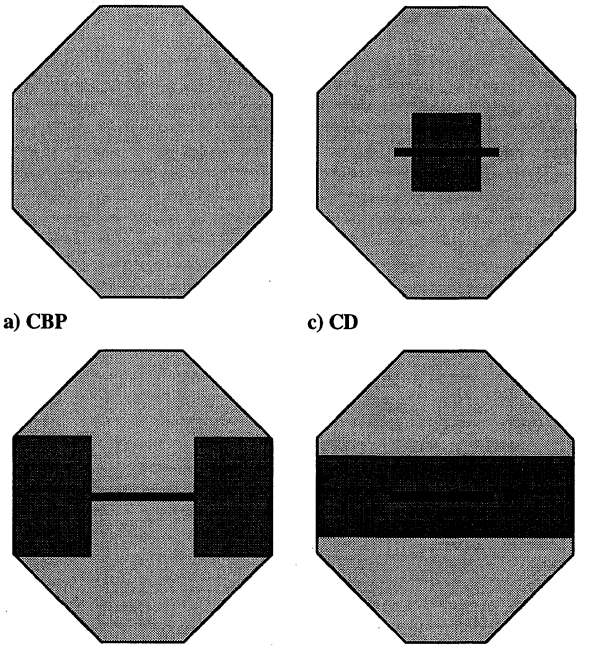

Fig. 3 Disbond configuration types.

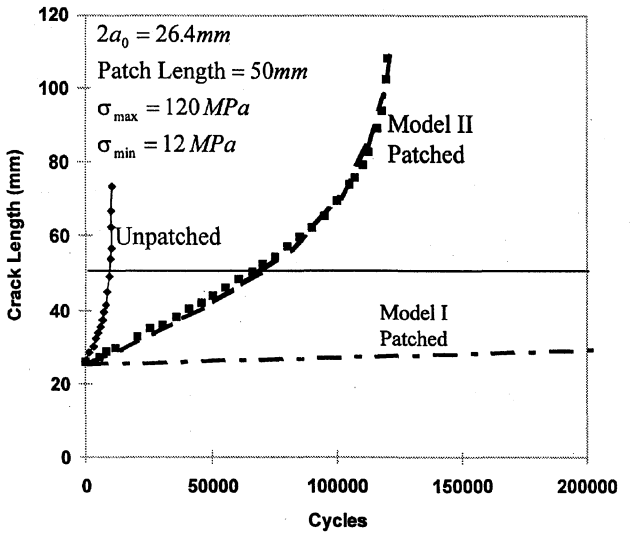

Fig. 4 Comparison of results from numerical models I and II with the experimental data for CPB: ♦, unpatched; ■, perfect patch; — –, linear model II; and — -, linear model I.

In the first configuration, there is no disbond in the patch repair. As has been determined from the Denney's experiment, the fatigue life of a perfectly patched specimen is about 10 times longer than the unpatched specimen, as shown in Fig. 4. However, using the material data (for the linear elastic shear modulus of the adhesive) provided in Denney,[1] it was found that the predicted fatigue life differs considerably from the experimental data for specimen 20. In the numerical model of the CPB, the predicted fatigue crack growth is notably slower than the experimental result, by a factor of approximately five (shown in Fig. 4 as linear model I). Because the material data for the boron/epoxy laminate and the aluminum panel are considered to be quite reliable, it would be easy to conclude that either the linear elastic adhesive model or the material data for the adhesive film is not accurate. By simple trial and error, it was found that, by reducing the shear stiffness K_{ADHE} of the adhesive layer, the predicted fatigue growth curve would correspond very well to the experimental result, as shown in Fig. 4 as linear model II. In this linear model II, the adhesive stiffness, $K_{ADHE} = 0.2 \times 10^{12}$ Pa/m (0.73×10^6 psi/in.), is an order of magnitude less than the adhesive stiffness calculated from the perfectly linear elastic material data, $K_{ADHE} = 2.9 \times 10^{12}$ Pa/m (10.6×10^6 psi/in.). The

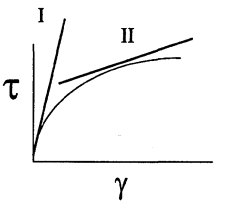

Fig. 5 Nonlinear material behavior of adhesive layer where the shear modulus is strongly dependent on the shear strain.

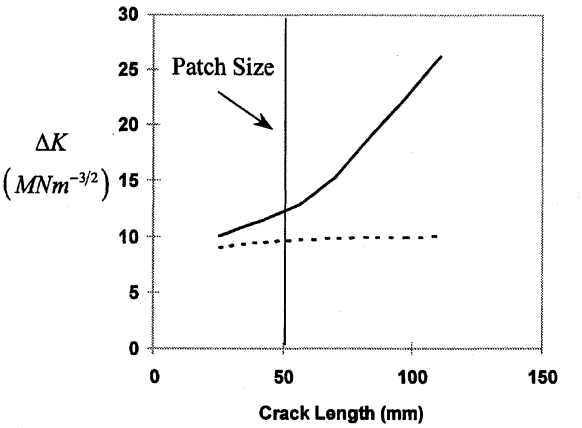

Fig. 6 Stress intensity factor as a function of crack length: ——, FEAM model and - - - -, Rose's model.

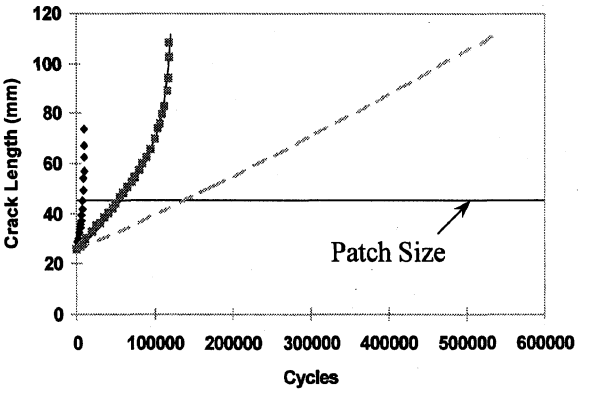

Fig. 7 Fatigue response based on FEAM and Rose's models: ♦, unpatched; ■, perfect patch; ——, FEAM model; and – – –, Rose's model.

difference in the adhesive stiffness between these two models can be partly attributed to the fact that the behavior of the adhesive material tends to be strongly nonlinear, as shown in Fig. 5. Thus, the use of the tangent shear modulus as in linear model II, i.e., slope of the nonlinear shear stress–strain level at the current average operating stress level in the adhesive, seems to be sufficient in predicting the fatigue response of a bonded repair. The value of the tangent shear modulus for linear model II, as surmised from fitting the fatigue growth data for specimen 20, will be used in the analysis of all the other remaining specimens. The validity of this approximation is borne out by the comparison of the analytical predictions for these other specimens with test data.

Unlike Rose's model,[4,5] which is only valid when the crack is much smaller than the size of the patch, the numerical model based on the FEAM was able to predict the fatigue response when the crack grows within the patch as well as when the crack grows outside of the patch. Figure 6 plots the stress intensity factor ΔK as a function of the crack length when calculated 1) based on the FEAM and 2) based on Rose's model.[4,5] In Fig. 6, both models are based on the same adhesive stiffness K_{ADHE} (material model II). When the crack size is small relative to that of the patch, the difference between these two models is about 10%. However, as the crack grows longer, the difference between these two models increases substantially, especially when the crack tip grows beyond the boundary of the patch. The difference between these two models is magnified even greater on the fatigue curve plotted in Fig. 7. Note that one of the assumptions in Rose's model,[3] as to the characteristic load-transfer length Λ, is not satisfied in this analysis. To obtain the asymptotic

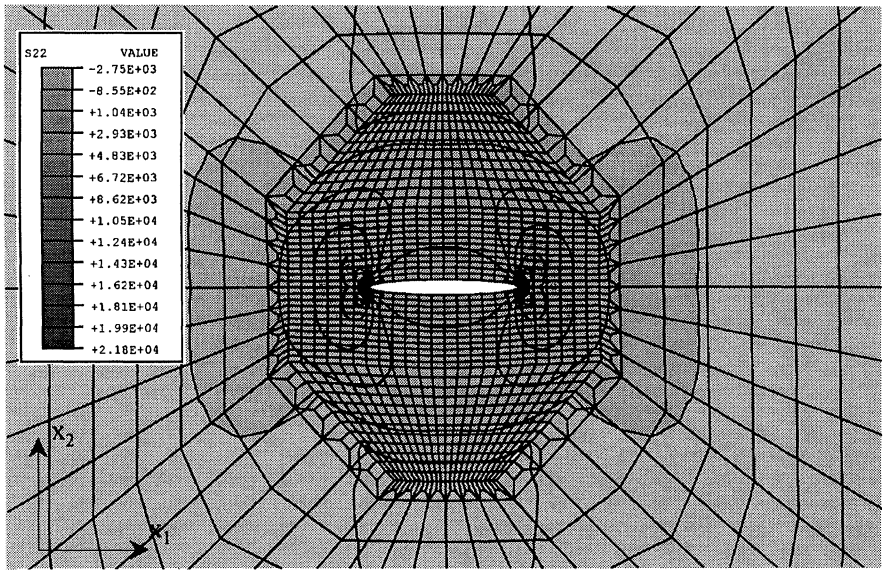

Fig. 8 Contour plot of the residual stress σ_{22} due to the curing process.

behavior of a crack under a composite patch, Rose had to assume that the load-transfer length has to be significantly smaller than the size of patch:

$$\Lambda = \left[\frac{G_{\text{adhe}}}{t_{\text{adhe}}}\left(\frac{E_{\text{patch}}t_{\text{patch}} + E_{\text{panel}}t_{\text{panel}}}{E_{\text{patch}}t_{\text{patch}}E_{\text{panel}}t_{\text{panel}}}\right)\right]^{\frac{1}{2}} \ll h_{\text{patch}} \qquad (4)$$

where E is the elastic modulus and h_{patch} is the height of the composite patch.

As described in an earlier section, the process of curing of the composite patch on the aluminum panel has been modeled. Because of the incompatibility in the coefficients of thermal expansion between the boron/epoxy patch and the aluminum panel, residual stresses would be induced when the temperature is dropped after the curing process. Figure 8 shows the contour plot of the residual stress σ_{22} in the aluminum panel generated after the panel has been cooled from the cure temperature of 121°C to the room temperature, 20°C. The deformed shape in Fig. 8 has been magnified by a factor of 100. Because the panel contracts much more than the composite patch, the crack surfaces would be opened by the residual stress generated, hence the resulting high stress concentrations on the crack tips, as shown in Fig. 8.

Unlike Rose's model where disbonds cannot be modeled, the FEAM can be used to predict the fatigue response of partially disbonded patches. Using the adhesive stiffness obtained from the perfect patched specimen, the fatigue response of a composite patch with CTD is analyzed. In this configuration, two specimens were tested: specimens 6 and 7. In both specimens, the disbond area is 20% of the patch area. Figure 9 shows that the predicted fatigue curve correlates very well the experimental data from specimens 6 and 7. Even though the disbond areas on both crack tips are quite large, both the analysis and the experiment show that the fatigue life of the specimens would be reduced by no more than 20%.

In the next analysis, the fatigue crack growth of specimens with a CD is evaluated. Specimen 16 has a disbond area of 10%, and specimen 17 has a disbond area of 5%. Figure 10 shows that the fatigue responses predicted with FEAM agree quite well with the experimental data from specimens 16 and 17. Because the fatigue life of specimen 16 (CD with disbond area of 10%) is less than that of specimen 6 or 7 (CTD with disbond area of 20%), it can be inferred that the effectiveness of the composite patch is more sensitive to the disbonds located at the center of the crack rather than the disbonds located at the crack tips.

Four FWD specimens have been investigated by Denney[1]: specimens 4, 5, 11, and 14. These specimens have disbond areas of 20% (for specimens 4 and 5), 10% (for specimen 11), and 5% (for specimen 14). The numerical analysis seems to provide good correlation with the experiment when the disbond area is small. However, for specimens with larger disbond area, the numerical solution seems

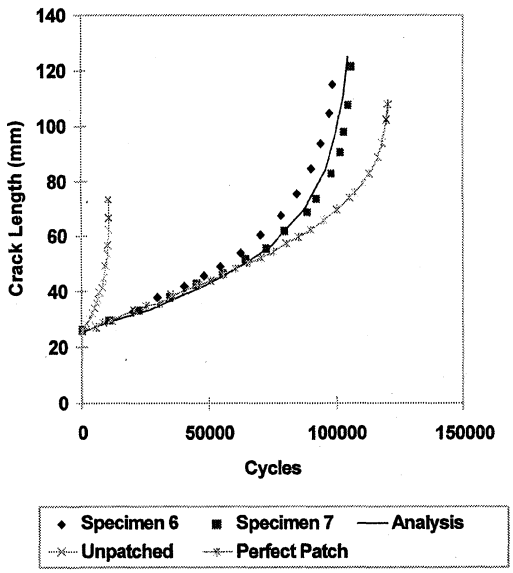

Fig. 9 Comparison of numerical result with experimental data for CTD.

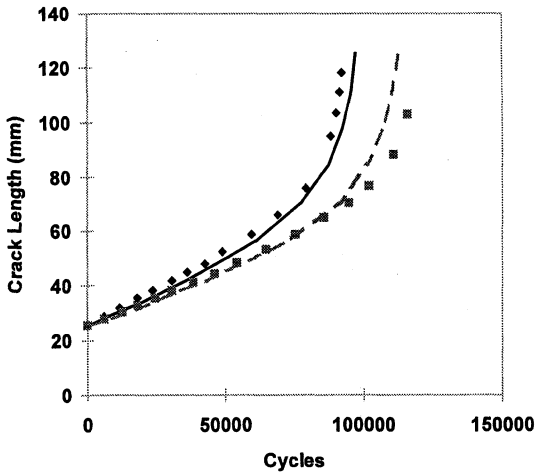

Fig. 10 Comparison of numerical result with experimental data for CD: ♦, specimen 16; ■, specimen 17; ——, analysis 16; and – – –, analysis 17.

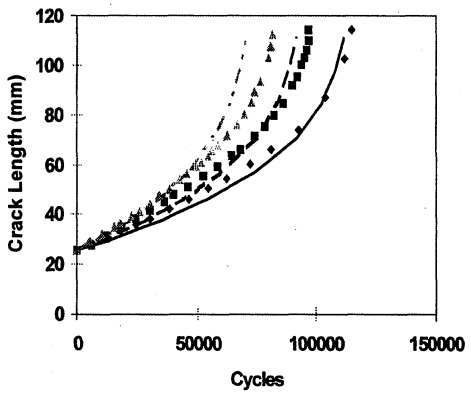

Fig. 11 Comparison of numerical result with experimental data for FWD: ♦, specimen 14; ■, specimen 11; ▲, specimen 5; ——, analysis 14; – – –, analysis 11; and – – –, analysis 5.

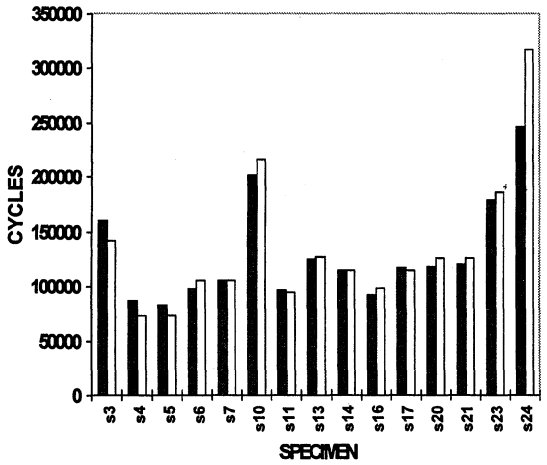

Fig. 12 Predicted fatigue lifes against the experimental data; cycles to failure: ■, experiment and □, analysis.

to over-predict the reduction in the fatigue life, as shown in Fig. 11. The predicted number of cycles to failure for specimens 4, 5, 11, and 14 are 73,404, 73,404, 95,048, and 115,108, respectively. These results correspond with the experimental data where the number of cycles to failure for specimens 4, 5, 11, and 14 are found to be 86,995, 82,324, 97,278, and 114,423, respectively.

To summarize the ability of FEAM in predicting the fatigue response of partially disbonded patch repair, the predicted results are displayed along with experimental data on a bar chart shown in Fig. 12. The parameters that are varied in these specimens include the disbond shape, the disbond area, the initial crack length, the maximum applied stress, and the applied stress ratio. The details of each specimen are given in Table 2. Figure 12 shows that, overall, FEAM can effectively predict the fatigue life of the aluminum panels with partially disbonded composite patches. The overall error of prediction is found to be 7.5%.

Effect of Temperature Cycles

In general, an aircraft would undergo a thermal cycle during each single flight. As the aircraft climbs to the cruising altitude, the ambient temperature can drop to less than −50°C. However, when the aircraft is parked in a depot under a hot sun, the temperature can rise to 70°C. Because the boron/epoxy patch has a lower thermal expansion coefficient, the patch would contract much less than the aluminum panel when the air temperature drops. This induces a cyclic thermal tensile loading on the crack tip at a time when the mechanical stress is highest. In the current analysis, the sensitivity of the adhesive stiffness to the temperature is not considered; however as pointed out in the earlier section, the initial stresses due to the curing process (at 121°C) are accounted for in this numerical model. Figure 13 shows the fatigue response of a CBP for case I, where the fatigue load is applied at room temperature, and case II, where the

Table 2 Details of the specimens modeled

Specimen	Configuration	Disbond area, %	Peak load, MPa	$R = \sigma_{min}/\sigma_{max}$
3	CBP	0	120	0.15
4	FWD	20	120	0.10
5	FWD	20	120	0.10
6	CTD	20	120	0.10
7	CTD	20	120	0.10
10	CBP	0	120	0.10
11	FWD	10	120	0.10
13	FWD	20	100	0.10
14	FWD	5	120	0.10
16	CD	10	120	0.10
17	CD	5	120	0.10
20	CBP	0	120	0.10
21	CBP	0	120	0.10
23[a]	CBP	0	120	0.10
24[a]	CBP	0	100	0.10

[a]Initial crack length 12.7 mm instead of 25.4 mm in other specimens.

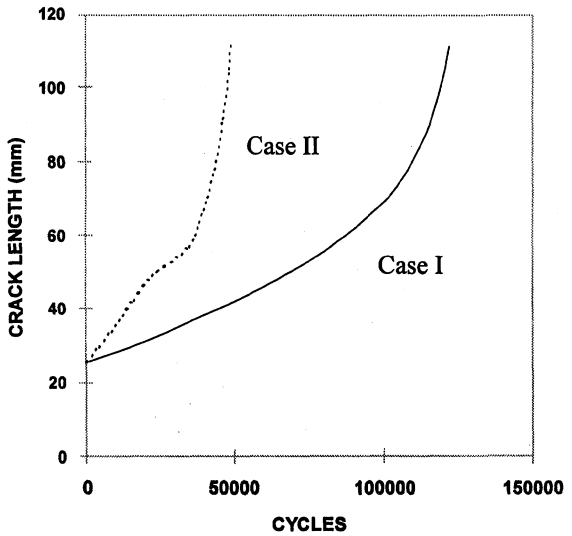

Fig. 13 Fatigue response of a CBP for case I where the fatigue load is applied at room temperature and case II where the maximum load σ_{max} is applied at −50°C and the minimum load σ_{min} applied at 70°C: ——, room temperature and - - - -, 50 to 70°C.

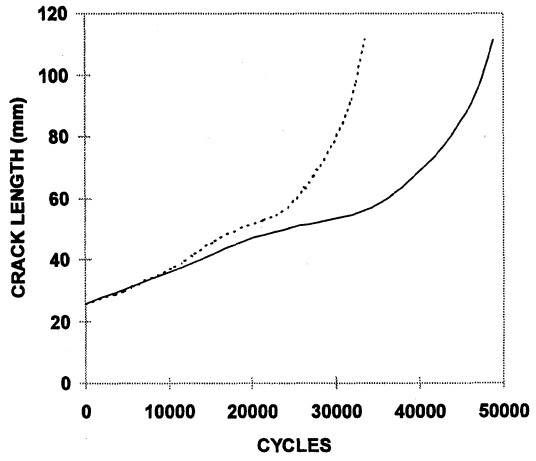

Fig. 14 Fatigue life of the specimen undergoing the thermal cycles with CTD: ——, perfect patch and - - - -, crack tip disbond.

maximum load σ_{max} is applied at −50°C and the minimum load σ_{min} is applied at 70°C. As shown in Fig. 13, the fatigue life of the specimen undergoing the thermal cycles would be reduced by more than 60% when compared to the specimen loaded at room temperature. Furthermore, it was found that when CTD is considered (where the disbond area is 20%), the fatigue life of the specimen undergoing the thermal cycles is further reduced by another 30%, as shown in Fig. 14. In contrast, the fatigue life of the CTD specimen loaded at

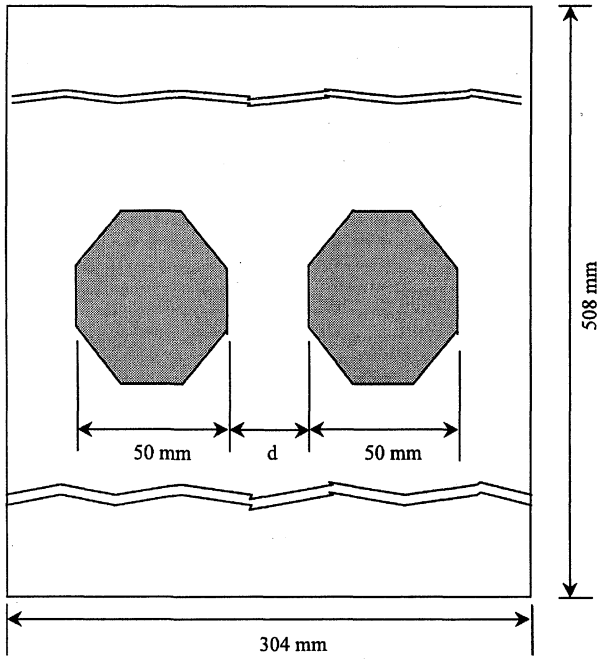

Fig. 15 Geometry of the aluminum patch with two patches lying horizontally.

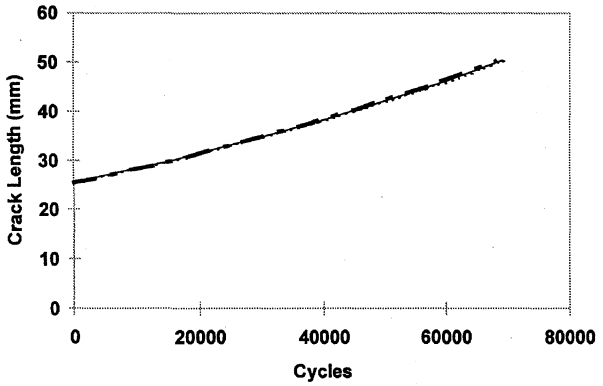

Fig. 16 Interaction of two patches lying on a horizontal line: ——, single patch; - - - -, two patches (d = 100 mm); and — —, two patches (d = 25 mm).

room temperature is reduced by no more than 20% when compared with a perfect patched specimen. This model seems to indicate that the specimen undergoing a typical thermal cycle would be more affected by partial disbond than the specimen loaded at constant temperature.

Interaction of Two Composite Patches

Given that cracks are sometimes found quite close to each other, it is important to study how two composite patches would interact. Two types of patch interaction are considered. In both configurations, the two patches are considered to be perfectly bonded. In the first configuration, both patches would lie on the same horizontal line (as shown in Fig. 15), the two cracks under the patches are collinear, and both the cracks are normal to the load direction. When the patches are 100 mm apart, there seems to be very little interaction between these two cracks. As shown in Fig. 16, the fatigue response of the specimen with two patches is quite similar to that of the specimen with a single patch. When the distance between the two patches is reduced to 25 mm, a similar fatigue response is found in which there is very little interaction between these two cracks, as shown in Fig. 16.

In the second configuration, both patches would lie on top of one another, in the loading direction, as shown in Fig. 17 (here the cracks are parallel to each other, one on top of the other, and both the cracks are normal to the load direction). When the patches are 100 mm apart, there seems to be very little interaction between these two cracks, as shown in Fig. 18. However, when the distance between

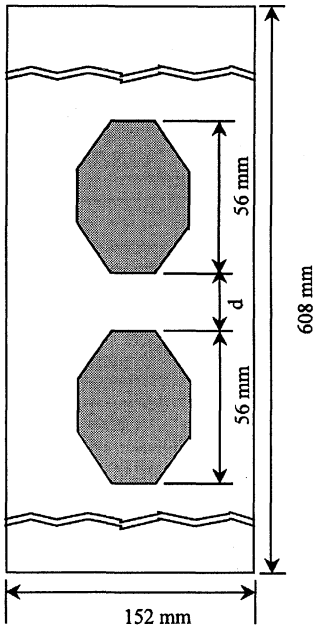

Fig. 17 Geometry of the aluminum patch with two patches lying vertically.

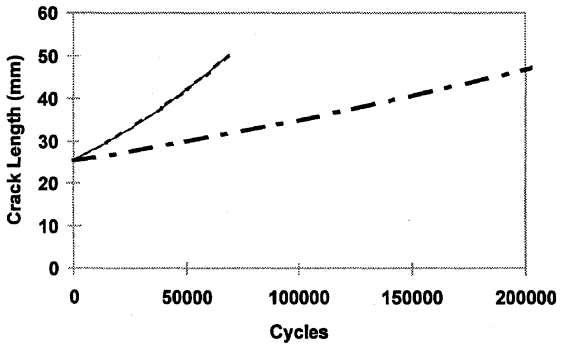

Fig. 18 Interaction of two patches lying on a vertical line: ——, single patch; - - - -, two patches (d = 100 mm); and — —, two patches (d = 25 mm).

the two patches is reduced to 25 mm, the fatigue crack growth is slowed by a factor of three, as shown in Fig. 18. Therefore, the specimen with two patches would have a longer fatigue life than the specimen with a single patch. However, it is possible that the metal in between the patches may fail in such situation; this is not considered here.

Conclusion

Numerical analyses based on the FEAM have been performed on several cracked panels with partially disbonded composite patches. The numerical results are compared with the experimental data obtained by Denney,[1] and the comparison indicates that the numerical results correlate quite well with the experimental data. Furthermore, a numerical study has been carried out to study the effect of high-stress low-temperature and low-stress high-temperature cycles. The result shows a very significant drop in the fatigue life when the specimen undergoes the thermal-fatigue cycle. This numerical result also shows that the specimen that undergoes the thermal-fatigue cycles is more sensitive to partial disbond than a specimen that undergoes the fatigue cycles at constant temperature. Furthermore, a numerical study has been carried out to examine the interaction between two nearby patches. It has been found that the interactions between two nearby patches do not reduce the fatigue life of the specimen.

Acknowledgments

This work was supported by the Air Force Office of Scientific Research, with Jim Chang as the cognizant program official. The technical assistance by Lehua Wang on the finite element alternating method is greatly appreciated.

References

[1]Denney, J. J., "Fatigue Response of Cracked Aluminum Panel with Partially Bonded Composite Patch," M.S. Thesis, Air Force Inst. of Technology, Dayton, OH, 1995.

[2]Jones, R., and Callinan, R. J., "Finite Element Analysis of Patched Cracks," *Journal Structural Mechanics*, Vol. 7, No. 2, 1979, pp. 107–130.

[3]Rose, L. R. F., "A Cracked Plate Repaired by Bonded Reinforcements," *International Journal of Fracture*, Vol. 18, No. 2, 1982, pp. 135–144.

[4]Rose, L. R. F., "Theoretical Analysis of Crack Patching," *Bonded Repair of Aircraft Structures*, edited by A. A. Baker and R. Jones, Martinus–Nijhoff, Dordrecht, The Netherlands, 1988, pp. 77–105.

[5]Fredell, R. S., "Damage Tolerant Repair Techniques for Pressurized Aircraft Fuselages," Ph.D. Dissertation, Faculty of Aerospace Engineering, Delft Univ. of Technology, Delft, The Netherlands, 1994.

[6]Mitchell, R. A., Wooley, R. M., and Chivirut, D. J., "Analysis of Composite Reinforced Cutouts and Cracks," *AIAA Journal*, Vol. 13, No. 6, 1975, pp. 739–749.

[7]Chu, R. C., and Ko, T. C., "Isoparametric Shear Spring Element Applied to Crack Patching and Instability," *Theoretical and Applied Fracture Mechanics*, Vol. 11, 1989, pp. 93–102.

[8]Tarn, J. Q., and Shek, K. L., "Analysis of Crack Plates with a Bonded Patch," *Engineering Fracture Mechanics*, Vol. 40, 1991, pp. 1055–1065.

[9]Park, J. H., Ogiso, T., and Atluri, S. N., "Analysis of Cracks in Aging Aircraft Structures, With and Without Composite-Patch Repairs," *Computational Mechanics*, Vol. 10, 1992, pp. 169–201.

[10]Nagaswamy, V., Pipkins, D. S., and Atluri, S. N., "A FEAM-Based Methodology for Analyzing Composite Patch Repairs of Metallic Structures," *Computer Modeling and Simulation in Engineering*, Vol. 1, No. 2, 1996, pp. 263–288.

[11]Roderick, G. L., "Prediction of Cyclic Growth of Cracks and Debonds on Aluminum Sheets Reinforced with Boron/Epoxy," *Fibrous Composite in Structural Design*, edited by E. M. Lenoe, D. W. Oplinger, and J. J. Burke, Plenum, New York, 1980, pp. 467–481.

[12]Baker, A. A., "Repair Efficiency in Fatigue Cracked Aluminum Components Reinforced with Boron/Epoxy Patches," *Fatigue and Fracture for Engineering Material and Structure*, Vol. 16, 1993, pp. 753–765.

[13]Nishioka, T., and Atluri, S. N., "Analytical Solution for Embedded Elliptical Cracks and Finite Element Alternating Method for Elliptical Surface Cracks, Subjected to Arbitrary Loadings," *Engineering Fracture Mechanics*, Vol. 17, 1983, pp. 247–268

[14]Atluri, S. N., and Nishioka, T., "Computational Methods for Three Dimensional Problems of Fracture," *Computational Methods in the Mechanics of Fracture*, edited by S. N. Atluri, North-Holland, Amsterdam, 1986, pp. 230–287.

[15]Rajiyah, H., and Atluri, S. N., "Evaluation of K-Factors and Weight Functions for 2-D Mixed-Mode Multiple Cracks by the Boundary Element Alternating Method," *Engineering Fracture Mechanics*, Vol. 32, 1989, pp. 911–922.

[16]Park, J. H., and Atluri, S. N., "Fatigue Growth of Multiple-Cracks near a Row of Fastener-Holes in a Fuselage Lap-Joint," *Computational Mechanics*, Vol. 13, 1993, pp. 189–203.

[17]Wang, L., and Atluri, S. N., "An Implementation of the Schwartz–Neumann Alternating Method for Collinear Multiple Cracks with Mixed Type Boundary Conditions," *Computational Mechanics* (to be published).

[18]Muskhelishvili, N. I., *Some Basic Problems of the Mathematical Theory of Elasticity*, Noordhoff, Gronigen, Germany, 1953.

[19]Park, J. H., "Improvement of the Accuracy of Stress Fields in Multiple Hole Crack Problems," Internal Rept., Computational Modeling Center, Georgia Inst. of Technology, Atlanta, GA, 1993.

[20]Forman, R. G., Kearney, V. E., and Eagle, R. M., "Numerical Analysis for Crack Propagation in Cyclic-Loaded Structures," *Journal of Basic Engineering*, Vol. 89, 1967, pp. 459–464.

[21]Atluri, S. N., *Structural Integrity and Durability*, Tech Science, 1977.

A. M. Waas
Associate Editor